Int. J. Nonlinear Anal. Appl. In Press, 1–13
ISSN: 2008-6822 (electronic)
http://dx.doi.org/10.22075/ijnaa.2021.23445.2541

Optimal demand response program design using a three phase optimization algorithm in electric vehicle charge/discharge application

Monireh Ahmadi[a,], Seyed Hossein Hosseini[b], Murtaza Farsadi[c]

[a]Department of Electrical Engineering, Malekan Branch, Islamic Azad University, Malekan, Iran

[b]Engineering Faculty, Near East University, 99138 Nicosia, North Cyprus, Mersin 10, Turkey

[c]Department of Electrical and Electronics Engineering, Engineering Faculty, Istanbul Aydin University, Istanbul, Turkey

(Communicated by Ali Jabbari)

Abstract

In this paper, the effects of distributed generation resources and demand response programs on the placement of charging or discharging stations are investigated. The effectiveness of an optimal exploitation approach is evaluated. pivotal factors of optimal charge/discharge power in stations are a combination of technical and economic parameters. The technical parameters contain minimization of network losses, voltage loss reduction in feeders, smoothing network load curve and harmonic elimination. The placement of stations and charge/discharge power were considered the most effective economic parameters. In other words, the minimization of charge/discharge operations results in cost reduction in purchasing power. A price-based demand-response program is considered to manage loads on the customer side and smooth the load curve. meta-heuristic optimization algorithms such as genetic algorithm (GA), particle swarm optimization (PSO), and imperialist are considered to find an optimal solution. This study is simulated on an IEEE standard 69-bus network. Using a conventional hybrid algorithm shows that the problem of station replacement and charge/discharge program can be solved optimally. Moreover, the effects of an increased number of stations and a disturbance in charge/discharge capacity are examined.

Keywords: Optimal placement, electric vehicles, meta-heuristic algorithms, demand-response program, distributed generation resources
2020 MSC: 82C70, 78A97

1 Introduction

Nowadays, the optimal establishment of charging/discharging stations and charging/discharging processes in electric vehicles (EVs) in the power grid has attracted the attention of the community of energy science engineers. One of the most important factors affecting the optimal placement of station programming is the demand-response program and load management on the customer side [8].

*Corresponding author
Email addresses: elec.ahmadi@gmail.com (Monireh Ahmadi), hosseini@tabrizu.ac.ir (Seyed Hossein Hosseini), murtazafarsadi@aydin.edu.tr (Murtaza Farsadi)

Received: April 2021 *Accepted:* June 2021

In Some studies, distributed generation resources are considered as auxiliary resources in the optimal demand response program for charging station establishment [7, 2, 4, 9, 1]. Furthermore, the capacity of distributed generation resources and locations of electric vehicle charging stations are determined by different optimized methods [3, 6, 5]. Moreover, Electric vehicle charging systems is designed inside microgrid and controlled vehicle-to-grid (V2G) interaction.

In this paper, the main objective is to obtain the optimal locations of electric vehicle charging stations in the network and investigate distributed generation resources on the proposed optimal demand-response program. a particular total objective function is proposed to reach desired technical and economic parameters.

2 Problem Formulation

Equation (2.1) defines the main performance index of this study with respect to the all of the concerned technical and financial parameters.

$$J_{\text{total}} = \sum_{n=1}^{5} j_n Q_n \tag{2.1}$$

where Q_n are weighting coefficients. In Eq.(2.2) J_1 represent the total losses in the network over a day.

$$J_1 = \sum_{t=1}^{24} \sum_{i=1}^{\text{Nline}} R_{\text{line}}\,(i)\,(I_{\text{line}}\,(\text{i},\text{t}))^2 \tag{2.2}$$

where Iline and Rline represent passing current and resistance of ith line at t-th hour, respectively.

In addition, in Eq.(2.3) J_2 represents the total voltage losses in the network over 24 hours (after incorporation of renewable energy resources).

$$J_2 = \sum_{t=1}^{24} \sum_{i=1}^{Nbus} |1 - \text{V}(\text{i},\text{t})| \tag{2.3}$$

where $\text{V}_{i,t}$ denotes the voltage at the i^{th} bus at the t^{th} hour. Moreover, J_3 is the energy consumption cost function which contains 3 main subsection as follow.

The cost of consumption in the network that needs to be paid to the distribution company. In the first step, according to the renewable energy resources and EV in the network, the input power provided by the substation at the t^{th} hour should be calculated as follows:

$$P_{sub}(t) = \sum_{i=1}^{Nbus} P_d(i,t) + \sum_{j=1}^{Nline} P_{loss}(i,t) - \sum_{k=1}^{Nstation} P_{disch}(k,t) + \sum_{k=1}^{Nstation} P_{ch}(k,t) - P_{wind}(t) - P_{pv}(t) \tag{2.4}$$

where:

- $P_{sub}(t)$: Input power provided by the substation at the t^{th} hour (kW)
- $P_d(i,t)$: Demand active power at the i^{th} bus and t^{th} hour (kW)
- $P_{\text{loss}}\,(i,t)$: Power losses in the i^{th} line at the t^{th} hour (kW)
- $P_{\text{disch}}\,(k,t)$: Discharged power from EV to the network at the k^{th} station and t^{th} hour (kW)
- $P_{ch}(k,t)$: Charged power from the network to EV at the k^{th} station and t^{th} hour (kW)
- $P_{\text{wind}}\,(t)$: Generated power in the wind section of the renewable energy production unit at th hour (kW)
- $P_{pv}(t)$: Generated power the renewable energy section like photovoltaic panels at th hour (kW)

- $Nbus$, $Nline$ and $Nstation$ are the number of busses, line, and electric vehicle charging/discharging stations in the network, respectively.

Regarding to Eq.(2.4) the sixth cost function can be introduced as Eq.(2.5). In Eq. (2.5), the constant coefficient (1.2) represents the profit share of the distributed energy company. In this case, it is assumed that the distribution generation company takes a $\sigma\%$ profit.

$$J_6 = \sum_{t=1}^{24}(1+\sigma)P_{sub}(t)C(t) \tag{2.5}$$

where C_t represents the cost of purchased energy by the distribution company at the t^th hour from the network power plant units. The energy prices per hour based on three situation of off-peak, average and peak are listed in table 1.

Table 1: Calculation of the profit offered to electric vehicle owners.

Period	Off-peak	Average	Peak
Hour	$23-9$	$10-18$	$19-23$
Power price per kW.h ($)	10	15	20
Price of power purchased by vehicle owners from distribution company per kW.h ($)	12	18	24
Price of power sold by vehicle owners to distribution company per kW.h ($)	11	16.5	22

Due to the presence of EVs in the network The charge/discharge costs at the stations contains two part:

1- The cost to be received from vehicle owners during the charging process at the stations

2- The cost to be paid to vehicle owners once discharging vehicle batteries to the network

The sum of these costs is calculated by Eq.(2.6). In Eq.(2.6) constant coefficient (μ) is a encouragement factor which means to encourage customers (EVs owners), the discharge cost paid to them is $\mu\%$ higher than the charge cost that the main network receives.

$$J_7 = \sum_{t=1}^{24}\left(C(t)\sum_{k=1}^{\text{Nstation}}P_{ch}(k,t) - (1+\mu)\cdot C(t) * \sum_{k=1}^{\text{Nstation}}P_{disch}(k,t)\right). \tag{2.6}$$

Table 1 It expresses this concept that the vehicle owners can purchase electrical energy during off-peak and average hours (when the energy price is lower) and sell it during peak hours (when the energy price is higher).

In the total cost function Eq.(2.1), J_3 is the sum of two mentioned cost function

$$J_3 = J_6 + J_7 \tag{2.7}$$

Since the parameters such as cost, power loss, and voltage loss which are used in the objective functions are different in nature, the objective function needs to be normalized by per-uniting these parameters relative to the initial state, when there is no electric vehicle charging station.

Moreover, J_4 stands for the total harmonic distortions of current and voltage over 24 hours of a day at charging station and Q_4 is the weighting coefficient considered for distortion. Therefore, J_4 is calculated as follows:

$$J_4 = \sum_{t=1}^{24}\sum_{i=1}^{\text{bus number}} TDD(i,t) + THD(i,t) \tag{2.8}$$

where TD $D(i,t)$ and THD(i,t) represent total demand distortions of current load and total harmonic distortion of voltage, respectively, at the i^{th} bus and t^{th} hour of the day. $TDD(i,t)$ and $THD(i,t)$ are calculated by (2.9) and (2.10), respectively.

$$TDD(i,t) = \left(\frac{8}{1500}\right)\cdot CH(i,t) \tag{2.9}$$

$$THD(i,t) = \left(\frac{5}{1500}\right)\cdot CH(i,t). \tag{2.10}$$

Due to the different nature of parameters in the cost function, J_5 parameters are per-united relative to their maximum values. The maximum values of J_5 can be achieved at the highest possible power of electric vehicle charging (1.5 MW for each station), at both stations in a day. In this study, it is assumed the charging power at the stations is based on IEEE519-1992 which is one of the standards that has addressed the harmonic distortion induced by electric vehicle charging. Equations (2.9) and (2.10) are introduced in the IEEE519-1992 standard regarding the reasonable maximum values of THD and TDD. In addition, a direct relationship is considered between the electric vehicle's charged/discharged power and harmonic distortion.

In Eq. (2.11), J_5 expresses the effects of constraints imposed by electric vehicle performance. If the constraints are satisfied, J_5 takes a zero-value.

$$J_5 = n_{\text{con}} * \eta \tag{2.11}$$

where n_{con} is the number of unsatisfied constraints and η is a constant value that is usually considered higher than the values of parameters of the main cost function. By J_4 the problem can be solved by meta-heuristic algorithms with respect to the constraints. The constraints imposed on the problem are as follows:

1) Charge/discharge power

The charge/discharge power at any station must be limited based on capacity of station at any time of day.

$$\begin{aligned} &0 \le \text{CH}(i,t) \le \text{Cap}(i) \qquad i = 1:n \\ &0 \le \text{DisCH}(i,t) \le \text{Cap}(i) \qquad i = 1:n \end{aligned} \tag{2.12}$$

where $\text{CH}(i,t), \text{DisCH}(i,t), \text{Cap}(i)$ denote the charge value, discharge value and capacity at the t^{th} station and t^{th} hour, respectively. n is the number of charging and discharging stations.

2) Difference of charge and discharge power

At a specified time in a day several charging and discharging devices are used for EVs at any station. The total exchanged electric power in these devices is limited by the total capacity of the station. Eq.(2.13) expresses constraint related to the sum of charge and discharge power.

$$0 \le CH(i,t) + \text{DisCH}(i,t) \le \text{Cap}_i, \quad i = 1:n \tag{2.13}$$

3) Prediction of the electric power exchange

The difference between total power charged to EV (from the network) and the total discharged power from the network (to electric vehicles) is expected to equate to the predicted power. In Eq.(2.14) this constraint is expressed:

$$\sum_{i=1}^{n} P_{Ch}(i,t) - \sum_{i=1}^{n} P_{DisCh}(i,t) = P_{\text{predic}}\ (t) \tag{2.14}$$

where $P_{\text{predic},\ t}$ is the predicted consumed-power for the set of EV at the th hour.

2.1 demand-response program

In the model of the proposed price-based demand-response program, load shift and load interruption can simultaneously occur. Moreover, by pricing consumption periods and transferring demand from peak to off-peak hours, the behavior of customers can be optimized. In the proposed program, customer satisfaction is related to the elasticity coefficient as follows:

$$e_{st} = \frac{\Delta L(s)/L_0(s)}{\Delta P(t)/P_0(t)} \left\{ \begin{array}{ll} e_{st} \le 0, & \text{if } s = t \\ e_{st} \ge 0, & \text{if } s \ne t \end{array} \right\} \tag{2.15}$$

where s is a time sequence ($\text{s} = 1, 2, 3, \ldots, \text{T}$) and other parameters are defined as follows:

$\Delta L(s)$: Variations in consumption load after implementing the proposed demand-response program

$L_0(s)$: Consumption load before the price-based demand-response program

$\Delta P(t)$: Variations in electricity price after implementing the proposed program

$P_0(t)$: Electricity price before the price-based demand-response program.

The costumers behaviour can be expressed in two situation in dealing with electricity price variation in different periods.

1) Self-elasticity loads

In the first situation, some essential loads (i.e., lighting loads) that cannot be used in other periods must be activated. Such loads that are sensitive only to one period are called self-elasticity loads. In this response, $s = t$ and only load interruption can occur and e_{st} is always negative.

2) multi-stage elasticity loads

In the second situation, some loads can be activated in off-peak periods instead of peak periods. Such behavior is called multi-stage elasticity and is evaluated by the cross-elasticity coefficient. In this response, $s \neq t$ and e_{st} is called cross-elasticity which is always positive. Eq.(2.16) shows the mathematical description of the problem.

The Load variations ($L(t)$) is calculated after implementing the price-based demand-response program by Eq. (2.16).

$$L(t) = L_0(t) \times \left\{ 1 + e_{st|s=t} \times \frac{[P(t) - P_0(t)]}{P_0(t)} + \sum_{\substack{s=1 \\ s \neq t}}^{24} e_{st} \times \frac{[P(s) - P_0(s)]}{P_0(s)} \right\}. \tag{2.16}$$

By using proposed program the profit made by selling electricity is not constant. Eq.(2.17) expresses the difference in profits before and after implementing the time-dependent load response program.

$$\pi_{PB} = P_0(t)L_0(t) - (P_0(t) + \Delta P(t))\, L(t). \tag{2.17}$$

In the demand-response program, the coefficient of load elasticity to temporal price variations has an important role in the calculations. The load elasticity coefficient that is concerned with the customers' reaction to price changes depends on some important parameters, including social, cultural, and economic subjects. The elasticity coefficient in this study is obtained from [8]. Due to the conventional three consumption periods, (i.e., off-peak, average, and peak,) 9 states are taken into account for the elasticity coefficient (Table 2).

Table 2: The coefficient of load elasticity to temporal price variations during different periods.

	Off-peak hours	Average hours	Peak hours
Off-peak hours	−0.2	0.008	0.006
Average hours	0.01	−0.2	0.008
Off-peak hours	0.012	0.016	−0.2

Since excessive load transfer to off-peak hours cause a new peak period the maximum allowable load variations in the demand-response program must be limited. In this paper, the maximum allowable load variations in the demand-response program were limited to 10% of the predicted initial load. In other words, loads are allowed to increase or decrease by 10% during different hours of the day.

3 Three Phase Optimal Demand-Respose Program

In this study, the standard 69-puls IEEE network is considered as the test network. In addition, GA, PSO, and imperialist competitive meta-heuristic algorithms are utilized to solve the problem mentioned in section 2. In the first stage, the problem is solved by the GA, and the achieved results are utilized as the input data for the PSO and imperialist competitive algorithms. Two renewable energy resources are assumed to be available on buses 61 and 63. In addition, the total power consumption by the set of EVs in the network is definite at each moment and included in the problem data. The uncertainty of renewable energy resources is ignored and the profile of electric power generation by wind and solar resources was assumed as shown in Fig.1.

It is considered that each renewable unit included both wind and solar resources. The maximum possible power in the entire wind and solar resources is considered 0.5MW for each one. Renewable energy resources are located using the GA to minimize power and voltage losses in the network.

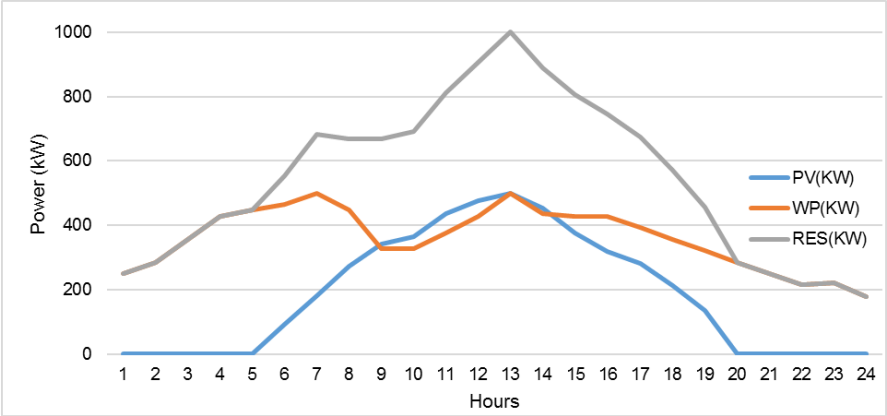

Figure 1: Generation power in the renewable energy resource (kW) at different times of the day.

In the concerned test network, two Ev charging stations are considered with a capacity of 1.5MW. Fig. 2 indicates the total consumed load by EVs.

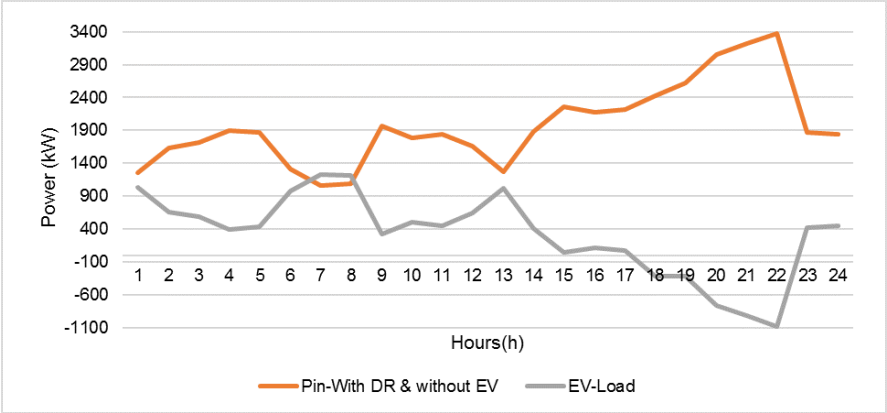

Figure 2: Electric vehicle consumption and other loads in the standard 69-bus IEEE network.

In Fig. 2, the negative amount of consumed power is actually the injected power by EVs (discharging). Similarly, a positive amount of consumed power by EV indicates that EVs are receiving energy from the network (charging). In the 69-bus network, if no renewable energy resource and EV is available, and the demand-response program is not implemented, the active power consumption in a day is 73MW. Otherwise, by considering two renewable energy resources, the demand for power supplied by the network decreases to 47MW. Because of considering two renewable energies, the base load is considered 47MW during 24 hours. Moreover, EVs were used such that the minimum frequency fluctuations and the smoothest load curve were reached. In other words, the behavior of EV with respect to the minimization of frequency deviation and the smoothing process of the load curve is programmed. In this study, the optimal placement of charging/discharging stations and optimal electric vehicle programming by GA, PSO algorithm, and imperialist competitive meta-heuristic algorithms are performed. The problem's total cost function was segregated into three main parts; then optimized each part was by one of the conventional algorithms. In the first stage, the optimization process is performed by the GA, then in the second phase PSO algorithm uses the results of GA as input data, and in the last section by considering the last phase result as input data, the imperialist competitive algorithm is utilized.

4 Simulation Results

Six scenarios are defined to investigate the effect of the demand-response program and distributed resources.

- A:

1) There are no renewable energy resources.

2) There is no demand-response program.

- B:

1) There are no renewable energy resources.
2) proposed demand-response program is utilized.

- C:

1) Two renewable energy resources (wind and solar) are used.
2) There is no demand-response program.

- D:

1) Two renewable energy resources (wind and solar) are used.
2) proposed demand-response program is utilized.

- E: Increase in the number of stations
- F: Increase in the capacity of devices

Fig. 3 to Fig. 10 illustrate the achieved results during the simulations of the last phase of the triple algorithm for six scenarios. Since the last phase includes all of the parameters of the total cost function, the figures illustrate the simulation results for the imperialist competitive section. In scenario F, the number of stations increased from 2 to 4. Moreover, the charging/discharging capacity of stations is raised from 1.5 to 1.8MW in scenario E. Fig. 3 shows the total cost function in the six scenarios.

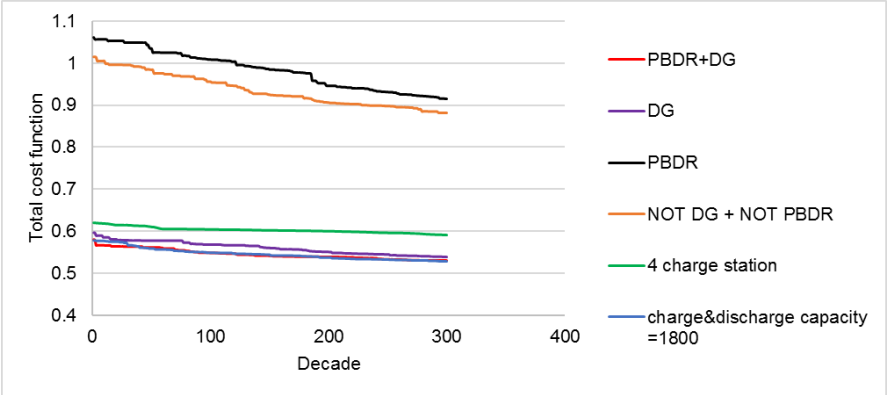

Figure 3: Objective function in in the last phase of algorithm algorithm.

As can be observed, the objective function offered a descending trend in all scenarios. In addition, the size reduction can be observed as the algorithm approached the optimal point. In scenarios in which the distributed resources are not corporate the size of the total cost function substantially increased in comparison with other situations. The objective function reaches the minimum optimal value in scenario D. Fig. 4 and Fig. 5 depict the charge/discharge cost curves during the last phase of the algorithm.

As can be observed in Fig. 4, In scenario B, EV charge costs are lower than in other states which shows the key role of DG in charge cost. On the other side, In scenario D, EV charge/discharge costs increased after 200 decades. By implementing the demand-response program, load activation is transferred from the peak to off-peak hours (i.e., smoothing of load curves). Therefore, the amount of electric vehicle charge/discharge would decrease which results in lower charge/discharge costs. Under the available conditions of the concerned network, as the load curve becomes more smoothed and the price difference becomes higher between different hours, power is bought in off-peak hours at a lower price in comparison with peak hours and it is sold in peak hours by EV owners to achieve a higher profit. The proposed demand-response program prevents load accumulation in peak hours and, thus, the demand is reduced in peak hours. Therefore, EVs have lower participation in the network (lower energy exchange). In scenarios with the presence of DG, a significant portion of the generated power by renewable resources which can be injected into the network. In these two cases, generated power can be purchased by vehicle owners in off-peak hours and sold in peak

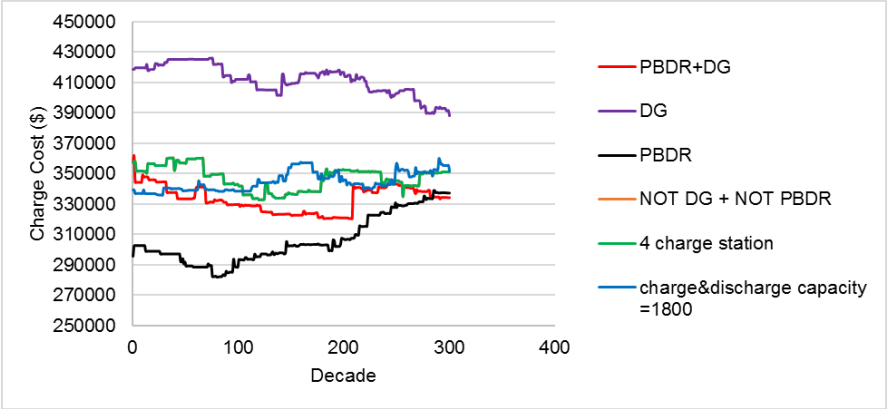

Figure 4: Electric vehicle charge cost in the last phase of algorithm.

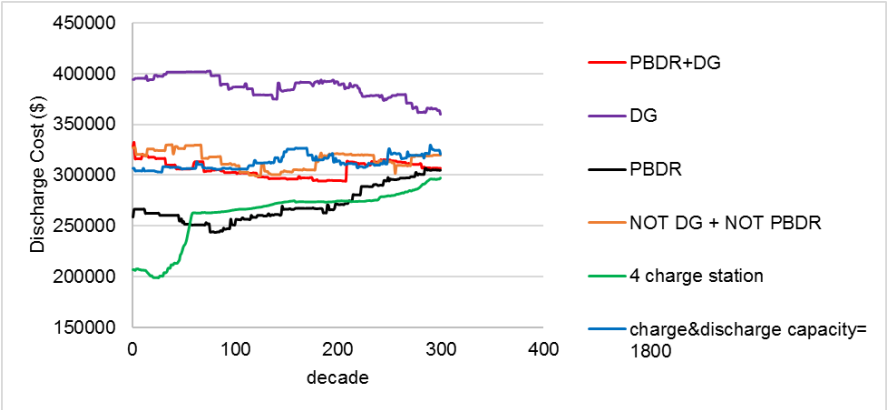

Figure 5: Electric vehicle discharge cost in the last phase of algorithm.

hours. Therefore, charge and discharge cost significantly increased compared to other states. In scenario D, charge and discharge costs are at the middle level (compared to scenarios B and C). Therefore, the increase in the number of stations and charge/discharge capacity changed charge and discharge costs negligibly.

The total cost in the last phase of the proposed three-phase algorithm is demonstrated in Fig. 6. As can be observed, in the absence of DG resources in the network, the total cost is considerably lower than that of other scenarios. Moreover, an insignificant effect on the total cost can be observed. In other words, in this situation, the required power should be purchased from the distribution company. Therefore, in these scenarios, the total cost is increased rapidly. Obviously, the increase in the number of stations yields falling costs as well. According to Fig. 4 and Fig. 5 and regarding the final optimal response, when there are four stations, the charging cost was higher compared to the discharge cost; as a result, the profit achieved by EV owners is reduced. Fig. 7 presents the voltage loss in the imperialist competitive phase algorithm. As can be observed, the absence of DG resources caused a rise in the voltage loss in the network, whereas the implementation of the proposed demand-response program degraded the conditions. In scenario C, the voltage loss is minimized. In scenario E, the increase in the number of charging and discharging stations resulted in the elevations of voltage loss in the network.

On the other side, the increase in the capacity of stations negligibly affected the voltage loss in this state.

Fig. 8 shows the power losses in the proposed program. Similar to Fig. 7, the absence of distributed generation resources yields an increase in power losses in the network. In scenario D, the minimum power losses are achieved in the network. In scenario F, the increase in the capacity of charging and discharging stations reduced power losses in the power grid; however, an increase in power losses is aroused due to the increase in the number of stations. Fig. 9 shows the input power to the network in the last phase of the proposed algorithm. As can be observed, purchased power from the distribution company is higher than that of the scenarios with distributed resources compared to scenarios with no DGs.

Fig. 10 illustrates the harmonic distortions induced by exploiting charging and discharging stations in the result

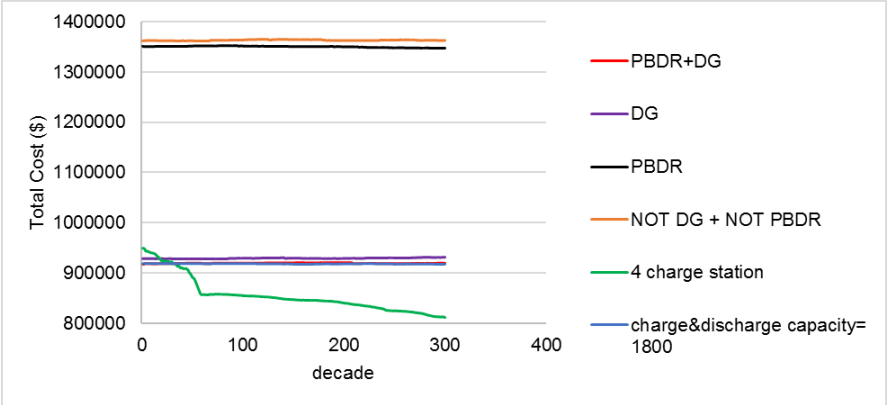

Figure 6: Total cost in the last phase of algorithm.

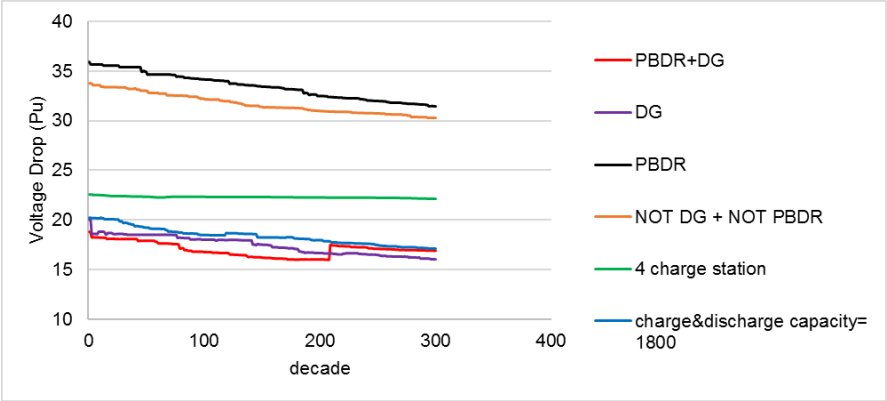

Figure 7: Voltage loss in last phase of algorithm.

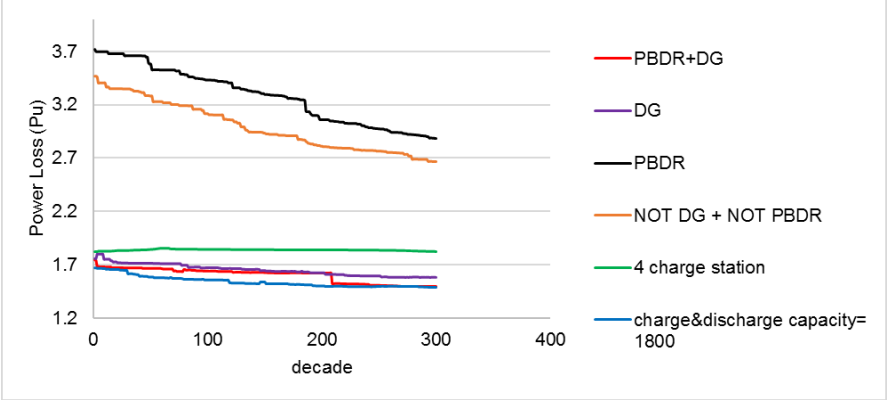

Figure 8: Power losses in last phase of algorithm.

of the algorithm. In scenario A, in absence of a demand response program and DGs, the energy exchange between the network and EV is raised causing elevated harmonic distortions induced by EVs. In scenarios with the implementation of the proposed demand-response program, a decrease in the harmonic distortions in the network is observable. In addition, in scenarios with an increase in the number and capacity of stations harmonic distortion reduction can be observed.

Table 3 lists optimal responses for the six scenarios which are achieved by the proposed optimal algorithm. In table 3, the optimal locations to establish charging and discharging stations in each scenario are predicted. As it is shown in scenario D, buses 4 and 61 are the optimal locations for the establishment of charging and discharging stations. In addition, in this study, by considering the absence of DG resources and a demand response program, the increase in

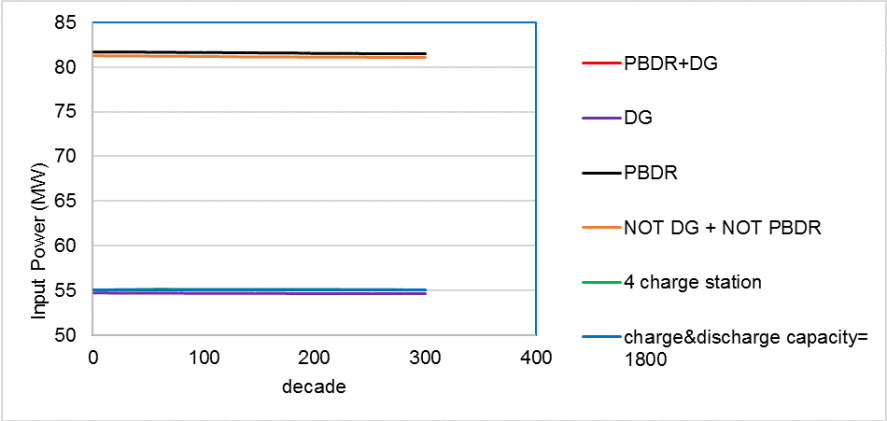

Figure 9: Input power in the imperialist competitive part of the triple algorithm.

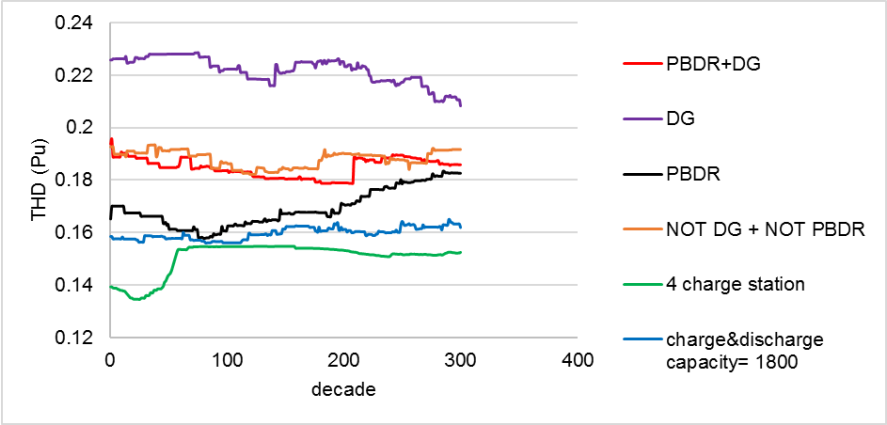

Figure 10: Harmonic distortions in the last phase of algorithm.

the capacity of charging and discharging stations is investigated. The results show there is no effect on the optimal placement of charging and discharging stations. Moreover, by an increasing the number of stations from 2 to 4, the previously predicted locations are not replaced, but discretely different locations as the optimal sites of stations are introduced.

Table 3: Comparison of the obtained results in different scenarios using proposed algorithm.

	Charge & Discharge Capacity =1800KW	4 Charge& Discharge Station	NOT DG + NOT PBDR	PBDR	DG	PBDR+DG
Optimal location to establish charging and discharging stations	61,4	6, 30, 39, 45	61,28	61,4	61,4	61,3
Charge cost ($)	334357	388000	337480	350985	216458.037	351950
Discharge cost ($)	307099.628	360257.1	304685.128	319540.628	296856.8279	320602.128
Total cost ($)	919160.1	931790.9	1346724	1362836.596	811419.8384	917932.58
Total input power (MW)	55.02123	54.65831	81.48381	81.04103024	55.10732505	55.01960271
Power losses (Pu)	1.4933476	1.583233	2.881383	2.666614767	1.819214132	1.48714782
Voltage loss (Pu)	16.87739888	16.0096	31.48372	30.31298945	22.12002535	17.10916962
THD (Pu)	0.18591	0.208132	0.182569	0.191506944	0.152446268	0.161840278

Fig. 11 to Fig. 14 show the optimal solution for the 24-hour charging/discharging programming at the two stations. As can be observed, the demand-response program had a notable impact on the optimal charging/discharging pattern at the stations' establishment. In scenario D, a different pattern for the optimal charging/discharging program at

the stations is suggested by the proposed method. However, in the three other scenarios (scenarios A, B, and C), identical behavior can be observed at the stations. Based on the results, using the proposed method for optimal charging/discharging program can affect reducing cost function size.

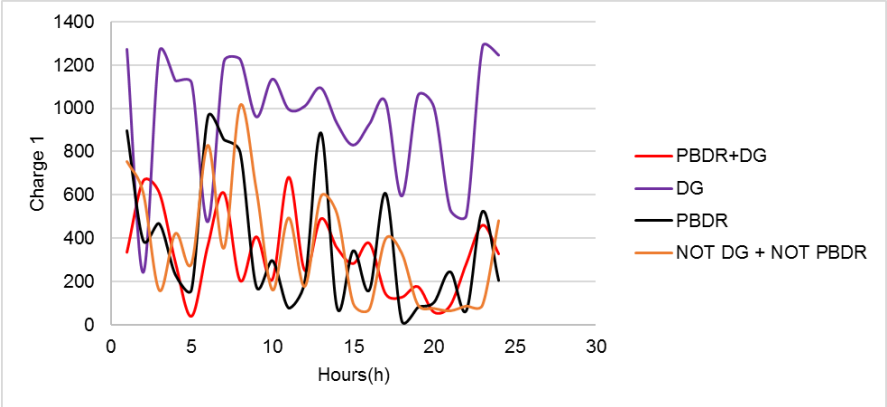

Figure 11: Optimal response as to the charging process at station No. 1 in different scenarios.

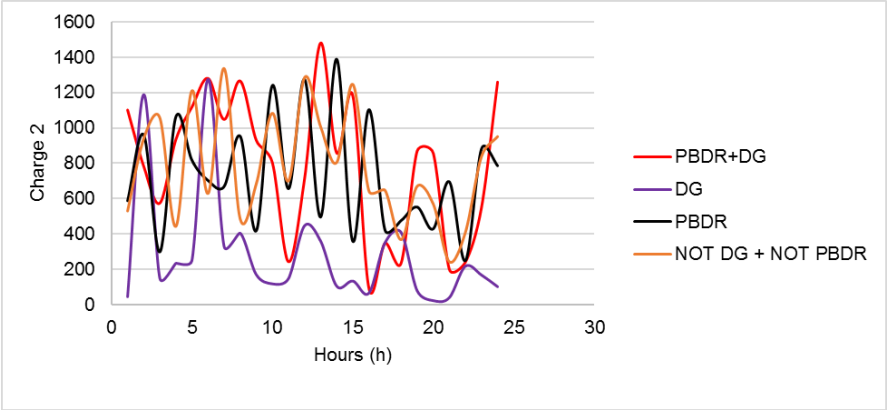

Figure 12: Optimal response as to the charging process at station No. 2 in different scenarios.

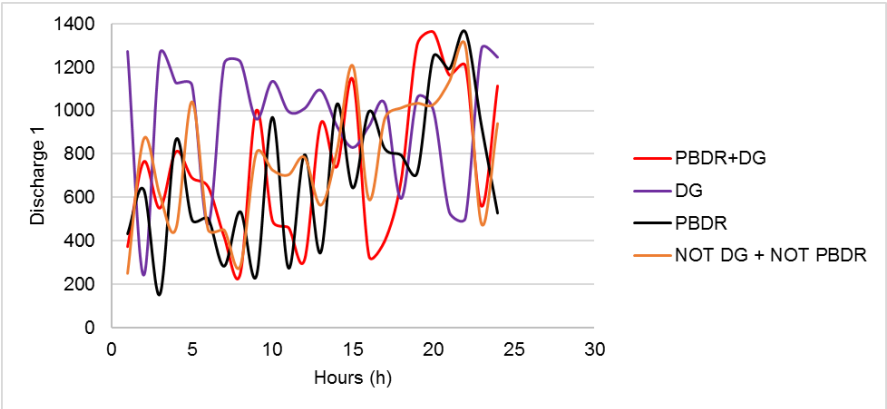

Figure 13: Optimal response as to the discharging process at station No. 1 in different scenarios.

5 Conclusions

This study has proposed an initial pattern for total charge and discharges power in the power grid. In this paper, a total cost function is considered to form an optimal solution for technical and economical parameters. The technical

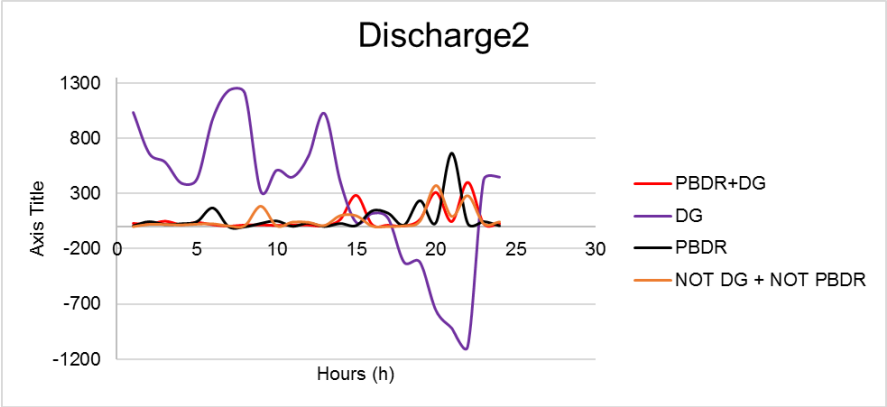

Figure 14: Optimal response as to the discharging process at station No. 2 in different scenarios.

parameters contain minimization of network losses, voltage loss reduction in feeders, smoothing network load curve and harmonic elimination. On the other side, the placement of stations and charge/discharge power are considered the most effective economic parameters. The proposed total cost function is used in three phases demand response program. In this particular method, GA, PSO and imperialist competitive algorithm are utilized as the first, second and third phases, respectively. In the proposed method the results of each phase are used as the input data for the next phase. The simulation is performed based on six scenarios which are relying on the absence/presence of DGs and demand response program. the proposed method is simulated on the standard 69-pulls IEEE network. The use of distributed generation resources has led to a decrease in the input power to the grid and as a result, the paper objectives are reached. reduction of power losses, voltage loss, and exploitation costs. The obtained results by the three algorithms have revealed almost the same charge and discharge at the stations and suggested identical sites to establish the stations. The genetic-imperialist competitive algorithm outperformed the other two algorithms, with fewer power losses and voltage losses. In this study, DGs such as wind and solar power show an improvement in total cost function minimization by the proposed method. Increasing the capacity of stations shows a significant effect on power loss reduction and voltage loss reduction, whereas an increase in the number of stations shows a negative effect of harmonic distortion.

References

[1] J.A. Domínguez-Navarro, R. Dufo-López, J.M. Yusta-Loyo, J.S. Artal-Sevil, and J.L. Bernal-Agustín, *Design of an electric vehicle fast-charging station with integration of renewable energy and storage systems*, Int. J. Electric. Power Energy Syst. **105** (2019), 46–58.

[2] O. Hafez and K. Bhattacharya, *Optimal design of electric vehicle charging stations considering various energy resources*, Renew. Energy **107** (2017), 576–589.

[3] M. Islam, H. Shareef, and A. Mohamed, *Optimal siting and sizing of rapid charging station for electric vehicles considering bangi city road network in malaysia*, Turk. J. Electric. Engin. Comput. Sci. **24** (2016), no. 5, 3933–3948.

[4] X. Jiang, J. Wang, Y. Han, and Q. Zhao, *Coordination dispatch of electric vehicles charging/discharging and renewable energy resources power in microgrid*, Procedia Comput. Sci. **107** (2017), 157–163.

[5] P.R.C. Mendes, L.V. Isorna, C. Bordons, and J.E. Normey-Rico, *Energy management of an experimental microgrid coupled to a v2g system*, J. Power Sources **327** (2016), 702–713.

[6] M.J. Mirzaei, A. Kazemi, and O. Homaee, *A probabilistic approach to determine optimal capacity and location of electric vehicles parking lots in distribution networks*, IEEE Trans. Ind. Inf. **12** (2015), no. 5, 1963–1972.

[7] G.R.C. Mouli, P. Bauer, and M. Zeman, *System design for a solar powered electric vehicle charging station for workplaces*, Applied Energy **168** (2016), 434–443.

[8] R. Sabzehgar, M.A. Kazemi, M. Rasouli, and P. Fajri, *Cost optimization and reliability assessment of a microgrid with large-scale plug-in electric vehicles participating in demand response programs*, Int. J. Green Energy **17** (2020), no. 2, 127–136.

[9] S. Tabatabaee, S.S. Mortazavi, and T. Niknam, *Stochastic scheduling of local distribution systems considering high penetration of plug-in electric vehicles and renewable energy sources*, Energy **121** (2017), 480–490.